Contrails, Cirrus Trends, and Climate

PATRICK MINNIS

Atmospheric Sciences, NASA Langley Research Center, Hampton, Virginia

J. KIRK AYERS, RABINDRA PALIKONDA, AND DUNG PHAN

Analytical Services and Materials, Inc., Hampton, Virginia

(Manuscript received 3 July 2003, in final form 28 October 2003)

ABSTRACT

Rising global air traffic and its associated contrails have the potential for affecting climate via radiative forcing. Current estimates of contrail climate effects are based on coverage by linear contrails that do not account for spreading and, therefore, represent the minimum impact. The maximum radiative impact is estimated by assuming that long-term trends in cirrus coverage are due entirely to air traffic in areas where humidity is relatively constant. Surface observations from 1971 to 1995 show that cirrus increased significantly over the northern oceans and the United States while decreasing over other land areas except over western Europe where cirrus coverage was relatively constant. The surface observations are consistent with satellite-derived trends over most areas. Land cirrus trends are positively correlated with upper-tropospheric (300 hPa) humidity (UTH), derived from the National Centers for Environmental Prediction (NCEP) analyses, except over the United States and western Europe where air traffic is heaviest. Over oceans, the cirrus trends are negatively correlated with the NCEP relative humidity suggesting some large uncertainties in the maritime UTH. The NCEP UTH decreased dramatically over Europe while remaining relatively steady over the United States, thereby permitting an assessment of the cirrus–contrail relationship over the United States. Seasonal cirrus changes over the United States are generally consistent with the annual cycle of contrail coverage and frequency lending additional evidence to the role of contrails in the observed trend. It is concluded that the U.S. cirrus trends are most likely due to air traffic. The cirrus increase is a factor of 1.8 greater than that expected from current estimates of linear contrail coverage suggesting that a spreading factor of the same magnitude can be used to estimate the maximum effect of the contrails. From the U.S. results and using mean contrail optical depths of 0.15 and 0.25, the maximum contrail–cirrus global radiative forcing is estimated to be 0.006–0.025 W m^{-2} depending on the radiative forcing model. Using results from a general circulation model simulation of contrails, the cirrus trends over the United States are estimated to cause a tropospheric warming of 0.2°–0.3°C $decade^{-1}$, a range that includes the observed tropospheric temperature trend of 0.27°C $decade^{-1}$ between 1975 and 1994. The magnitude of the estimated surface temperature change and the seasonal variations of the estimated temperature trends are also in good agreement with the corresponding observations.

1. Introduction

Condensation trails, or contrails, generated from high-altitude aircraft exhaust may affect climate because they can persist for many hours. Like their natural counterparts, these anthropogenic cirrus clouds reflect solar radiation and absorb and emit thermal infrared radiation causing a radiative forcing that depends on many factors, especially contrail optical depth and coverage (Sassen 1997; Meerkötter et al. 1999). Cloud radiative forcings are balanced by changes in variables such as surface and atmospheric temperatures, cloud cover, and precipitation (Hansen et al. 1997). Instantaneously, contrail radiative forcing can warm the atmosphere and warm or cool the earth's surface, apparently reducing the diurnal range of surface temperature (Travis et al. 2002). Although highly variable and uncertain, this forcing is generally positive when averaged over time (Minnis et al. 1999; Ponater et al. 2002; Meyer et al. 2002), resulting in a net warming of the troposphere and surface (Rind et al. 2000). The expected 2%–5% per annum growth (Penner et al. 1999) of worldwide jet air traffic through 2050 necessitates a more accurate assessment of contrail climate effects.

Current estimates of contrail radiative forcing only consider linear contrails young enough to be differentiated from natural cirrus clouds in satellite images. Those diagnoses of radiative forcing represent the minimum impact because they do not include the additional cloud cover resulting from the spread of aging linear contrails into natural-looking cirrus clouds (Minnis et al. 1998; Duda et al. 2001) and from any other cirrus

Corresponding author address: Dr. Patrick Minnis, NASA Langley Research Center, MS 420, Hampton, VA 23681.
E-mail: p.minnis@nasa.gov

clouds initiated by aerosols generated from aircraft exhaust (Jensen and Toon 1994). To reduce the uncertainty in the climatic effects of aircraft-induced cirrus clouds, it is necessary to determine the maximum change in cirrus coverage due to the combination of linear contrails and the cirrus clouds derived from them and from exhaust aerosols (Penner et al. 1999). The ratio of that combination to the linear contrail coverage is denoted as the spreading factor f_s.

Increases in cirrus coverage or decreased sunshine have been linked to jet air traffic over parts of the contiguous United States (see Changnon 1981; Sassen 1997) and Alaska (Nakanishi et al. 2001) for many years. Trends in regional cirrus frequency of occurrence are strongly correlated with high-altitude airplane fuel consumption between 1982 and 1991 (Boucher 1999). Previous studies confirm the expected outcome of increased air traffic, but are limited to small regions or to time periods too short for minimizing the impact of the 11-yr cycle in cloud cover (Udelhofen and Cess 2001). In this study, a 25-yr surface observation dataset is used to examine the longer-term global trends in cirrus amounts, relate them to the expected contrail coverage to estimate f_s, and then compute the maximum regional contrail-induced radiative forcing and regional temperature changes.

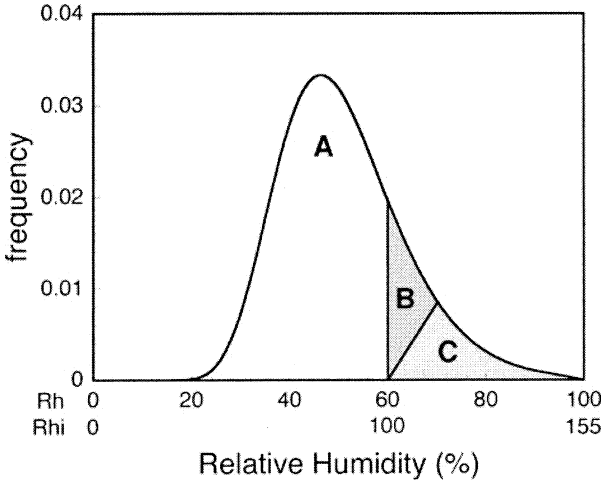

FIG. 1. Hypothetical annual relative humidity probability distribution at flight altitudes with $T = -50$°C. Neither persistent contrails nor cirrus clouds would occur for Rhi $< 100\%$ (area A). Cirrus clouds and persistent contrails can form when Rhi $> 100\%$, but the probability of forming cirrus through natural nucleation processes increases as humidity rises (area C) leaving the potential for development of additional cirrus coverage from contrails (area B) via nucleation from mixing of moist jet engine exhaust with ice-saturated ambient air. The portion of area B that is converted from clear air to cloudy air should rise as the cumulative flight path length increases over a given area with growing air traffic. Areas B and C correspond to Rh between 60% and 100%.

2. Background

Contrails occupy a fairly special niche in atmospheric thermodynamics because they form and produce ice clouds at ambient relative humidities that are less than those required for most natural cirrus cloud formation (Gierens et al. 1999). The presence of cirrus or persistent contrails depends on many factors such as temperature T, humidity, vertical velocity, and cloud condensation and freezing nuclei. The primary variable, however, is relative humidity. The complex dynamical processes initiating cirrus formation ultimately must produce the necessary water vapor. The most familiar moisture variable, relative humidity with respect to liquid water (Rh), is measured with radiosonde-borne hygrometers and used in weather analyses. For cirrus processes, the relative humidity with respect to ice (Rhi) is the relevant quantity. It exceeds Rh for a given specific humidity at $T < 0$°C. For $T < -39$°C, Rh $> 100\%$ typically corresponds to Rhi $> 150\%$. Although cirrus clouds form naturally through heterogeneous or homogeneous nucleation at low temperatures when the ambient Rhi is around 140%–160% (Sassen and Dodd 1989), or less when the air contains many nucleation aerosols (Ström et al. 2003), they will persist as long as Rhi exceeds 100%. Contrails can form and develop into cirrus clouds when $T < -39$°C and Rhi $> 100\%$ because, in many instances, aircraft exhaust temporarily raises the local Rh above 100% as it mixes with the ambient air causing nucleation of liquid droplets that freeze instantly. Therefore, contrails can add to the natural cirrus coverage when $T < -39$°C and Rhi $> 100\%$ and no natural cirrus cloud is already present (Fig. 1). If Rhi $< 100\%$, contrails can form but will not persist.

At flight altitudes, conditions that can support contrail-generated cirrus clouds exist 10%–20% of the time in clear air and within existing cirrus (Gierens et al. 1999; Jensen et al. 2001). Additionally, cirrus may form at lower supersaturations on aerosols derived from jet aircraft than on aerosols from natural sources (Jensen and Toon 1994). Therefore, high-altitude air traffic has the potential for increasing cirrus coverage and thickening existing cirrus clouds by generating additional ice crystals. If other relevant variables are steady over time, then cirrus coverage should increase where air traffic is significant.

3. Data

The surface-based cloud data consist of quality-controlled surface synoptic weather reports from land stations and ships filtered by Hahn and Warren (1999). Reports from automated weather stations and those with obvious errors and inconsistencies were eliminated from the dataset. The filtered observations include amounts for low, middle, and high clouds as well as associated weather conditions, solar zenith angle, and relative lunar illuminance. Values of frequency of occurrence, amount-when-present, and total cloud amount were calculated using the methods outlined in Hahn and Warren (1999). The cirrus amount is calculated by multiplying

TABLE 1. Boundaries of the air traffic regions (ATR). Land–other regions (LOR) and Ocean–other regions (OOR) consist of any land or ocean area that is not contained in any of the other land or ocean ATRs, respectively.

ATR	Latitude	Longitude
Western Asia (WASIA)	35°–70°N	90°E–180°
Europe (EUR)	35°–70°N	30°W–40°E
Western Europe (WEUR)	40°–60°N	10°W–15°E
United States of America (USA)	30°–50°N	50°–130°W
Land–other regions (LOR)	70°S–70°N	180°
North Atlantic (NA)	35°–70°N	70°W–20°E
North Pacific (NP)	35°–70°N	120°E–110°W
Ocean–other regions (OOR)	70°S–70°N	180°

amount-when-present by frequency of occurrence, a computation that implicitly assumes that the clouds are randomly overlapped. Annual and seasonal mean cirrus and total cloud amounts were calculated over land and ocean regions between 1971 and 1995. The original surface-based cloud dataset includes 1996. However, the number of surface stations in the United States gradually declined from 225 in 1971 to 110 in 1995. It dropped to 20 in 1996, drastically affecting the sampling patterns. Thus, only data prior to 1995 were used here to ensure that the data were a fair representation of the country as a whole.

Data from multiple stations within a single grid-box for a given month were averaged first for each site and then with the means from the other stations to yield a monthly grid box average. Annual means for land were calculated for 3° grid boxes having a minimum of 60 valid observations and 10 valid upper-level cloud observations for a minimum of 15 yr. Annual means for ocean were calculated for 5° grid boxes having a minimum of 30 valid observations and 5 valid upper-level cloud observations per month with a minimum of 7 months of data per year. Only data taken between 70°N and 70°S were used to calculate averages for the air traffic regions that are defined in Table 1.

Monthly mean cirrus and cirrostratus fractions from the International Satellite Cloud Climatology Project (ISCCP; Rossow and Schiffer 1999) D2 dataset were summed to provide total cirrus coverage (CCI) on a 250 $\times$ 250 km^2 grid for 1984–96 as a consistency check on the surface observations. Only daytime data taken between July 1983 and June 1991 and between July 1993 and June 1996 were used here to minimize the impact of the Mount Pinatubo eruption on the satellite retrievals. The CCI averages were computed using only the same grid boxes that were included in the surface air traffic region analyses.

Annual mean relative humidities with respect to liquid water at 300 hPa were computed on a 2.5° grid from the National Centers for Environmental Prediction (NCEP) reanalyses. RH(p) is used to indicate the annual mean computed from the instantaneous values, Rh(p) at pressure p. For brevity, the variable RH3 is used to represent RH(300 hPa). RH3 values are used to evaluate the changes in upper-tropospheric humidity (UTH) that can affect cirrus variability (Kistler et al. 2001). The mean annual distribution of expected linear contrail coverage (ECON) on a 2.8° grid is based on a parameterization of contrail formation tuned to satellite observations of linear contrails using air traffic data from 1992 and applied to 10 yr of global numerical weather analyses of relative humidity and temperatures at selected pressure levels (Sausen et al. 1998). The air traffic data are based on the assumption of great circle routes between two airports.

4. Results and discussion

a. Cirrus trends

Linear trends, $\Delta CC/\Delta t$, in annual mean cirrus coverage (CC) with time, t, were computed for each grid box having averages for more than 15 yr. Values of CC increased over the United States, the North Atlantic and Pacific, and Japan (Fig. 2a), but dropped over most of Asia, Europe, Africa, and South America. Increases are also evident around coastal Australia, sub-Saharan western Africa, and over the South Atlantic west of Africa. Areas with no trends were insufficiently sampled. Many of the trends are statistically significant at the 90% confidence level (Fig. 2b). The largest concentrated increases occurred over the northern Pacific and Atlantic and roughly correspond to the major air traffic routes reflected in the ECON distribution (Fig. 2c). Increased CC over the United States and around Australia and Japan coincides with relatively well-traveled routes. Over Europe, the CC trends are mixed, while $\Delta CC/\Delta t$ is negative over South American routes. The coincident NCEP RH3 dropped dramatically over Europe and northeastern Asia and less so over the northeastern United States, much of Asia, and the temperate ocean regions (Fig. 2d). RH3 rose over much of the Tropics, northern China, and southwestern United States and adjacent waters.

Although there appears to be close correspondence between many air traffic routes and increased CC, some differences exist between the local maxima in $\Delta CC/\Delta t$ and ECON. Assuming that contrails caused the changes in CC, then such differences could arise from slight discrepancies in gridding, idealization of air routes, and contrail movement. Contrails often advect hundreds of kilometers as they develop. Thus, their region of origin may differ from the area with maximum change in CC. To reduce this regional noise, the data were grouped into larger areas of contrail influence. The boxes in Fig. 2c show the air traffic regions while the remaining areas constitute the other-region categories (see Table 1). The western European region (WEUR) is a subset of the European region (EUR). If contrails induce more cirrus coverage, then the largest effects should occur over the United States and WEUR where ECON is greatest (Table 2).

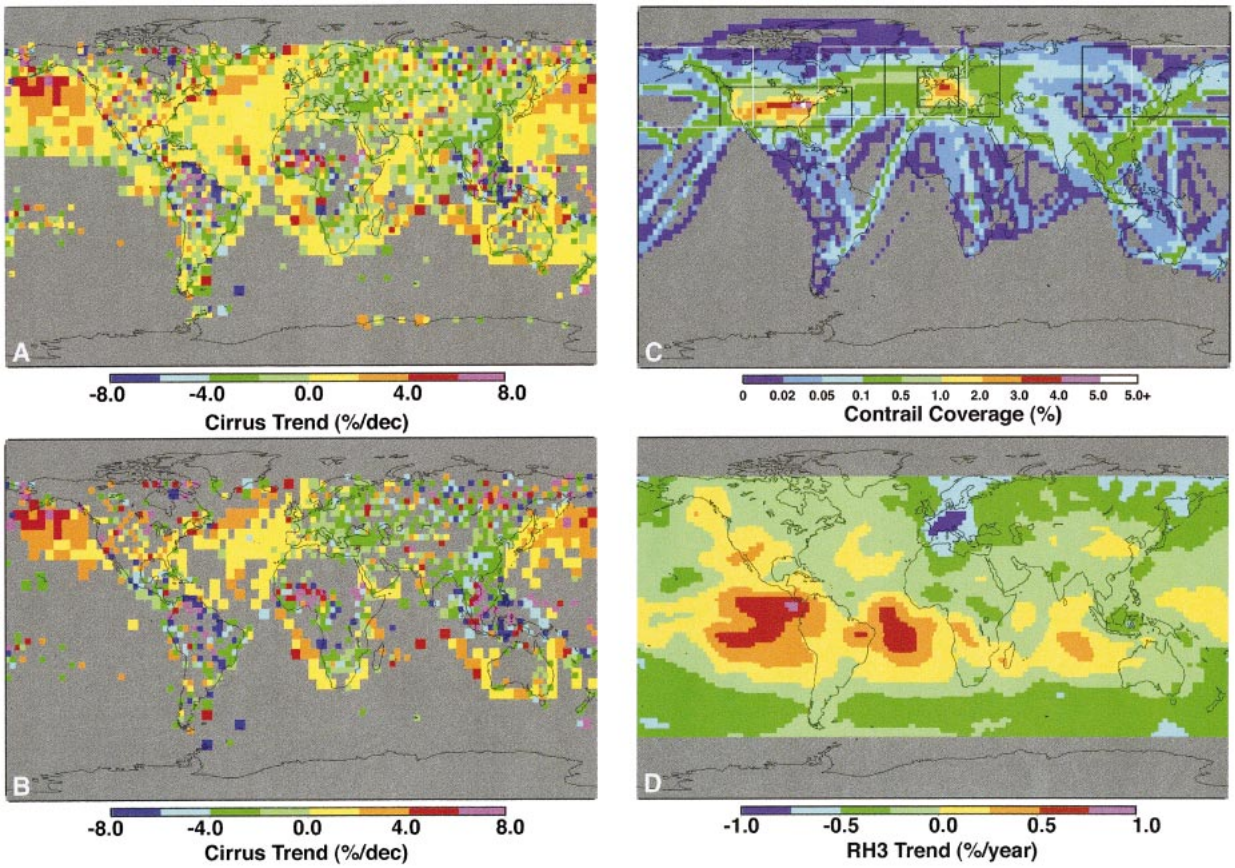

FIG. 2. Trends in cirrus coverage and 300-hPa relative humidity (1971–95) and estimated 1992 linear contrail coverage. (a) Trends in cirrus coverage for all regions with more than 15 yr of data. (b) Subset of (a) for all regions having trends significant at the 90% confidence level according to Student's *t* test. (c) Estimated linear contrail coverage. Black and white boxes determine the boundaries for the land and ocean air traffic regions, respectively. Only observations taken from land stations and from ships are used for the land and ocean air traffic regions, respectively. (d) Trends in annual mean NCEP relative humidity at 300 hPa.

The yearly air traffic region CC averages (Fig. 3) rose over the United States, remained steady over WEUR, and decreased over EUR, western Asia (WASIA), and the land–other regions (LOR), which include all land areas not included in the land air traffic regions. Values of CC also increased over the North Pacific (NP) and North Atlantic (NA) as well as over the ocean–other regions (OOR). Interannual variability in CC (Table 2) is greatest over Europe and least over the LOR. Trends in CC computed from the data in Fig. 3 are mostly of the same sign as the total cloud cover trends (Table 2) and can account for most of the total cloud cover change over WASIA, the LOR, and the NP. The increase in CC over the United States is compensated by slight decreases in other cloud types, while the opposite is true for EUR. Because CC is based on the assumption of

TABLE 2. Contrails, mean cirrus cover, and cloudiness trends (% decade^{-1}) over air traffic regions from surface (CC) and ISCCP (CCI) data. The numbers in parentheses indicate the interannual variability in CC. The 1971–75 trends in CC are all significant at the 99% confidence level, except over WEUR where no trend is apparent.

Region	1992 ECON (%)	Mean CC 1971–95 (%)	CC trend 1971–95	Total cloud trend 1971–95	CC trend 1983–95	CCI trend 1983–95
WASIA	0.08	36.2 (1.0)	−0.9	−0.7	−2.0	−2.1
EUR	0.60	18.5 (1.3)	−1.2	−0.4	−0.4	0.0
WEUR	1.52	19.8 (1.4)	0.0	−0.7	1.8	0.9
USA	1.75	29.2 (1.1)	1.0	0.5	0.3	2.3
LOR	0.09	24.5 (0.5)	−1.6	−1.4	−1.5	−0.6
NA	0.32	15.3 (0.7)	0.7	0.0	0.3	0.2
NP	0.16	15.7 (0.8)	0.9	0.8	1.6	−0.4
OOR	0.13	14.4 (0.6)	0.7	1.2	0.8	0.1

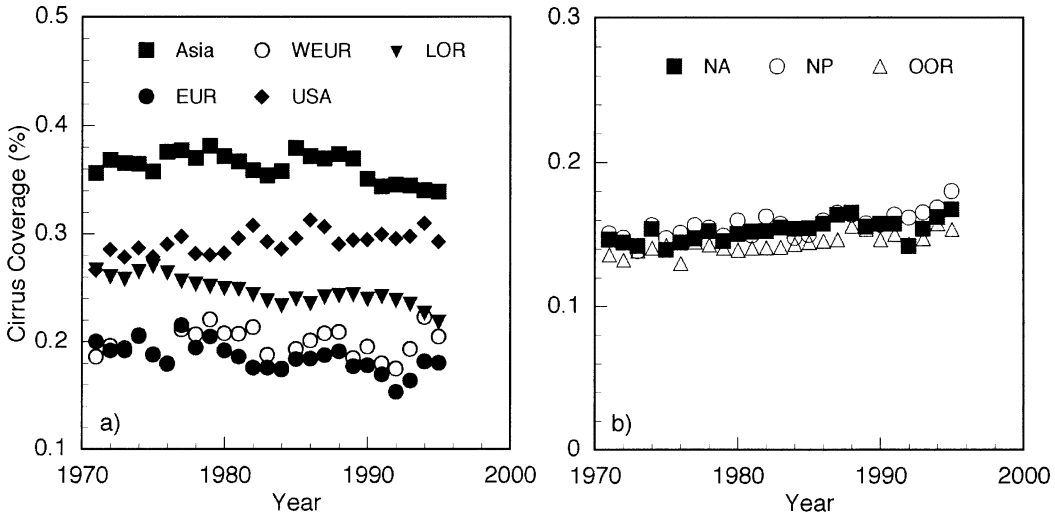

FIG. 3. Annual variation of CC over (a) five land regions [WASIA, WEUR, LOR, ERA, and United States (USA)] and (b) ocean regions (NA, NP, and OOR).

random overlap, that is, CC = Ci(1 + OC), the total cloud coverage is

$$\mathrm{TC} = \mathrm{Ci} + \mathrm{OC}, \tag{1}$$

where OC is other cloud coverage and Ci is the actual observed cirrus coverage. Using the original annual means of CC and TC for the United States, it can be shown that OC decreased by only 0.65% between 1971 and 1995, while Ci rose from 20.1% to 21.9%. Thus, the trend in OC is only -0.3% decade^{-1}. Over WEUR, the 0.7% decade^{-1} drop in total cloudiness is likely due to a decrease in low and midlevel cloud cover because CC remained constant. Total cloudiness increased more than CC over the OOR while $\Delta\mathrm{CC}/\Delta t$ over the NA appears to have been compensated by decreases in other cloud types.

The growth in ISCCP cirrus coverage over the United States greatly exceeds that from the surface observations (Table 2). Conversely, the CCI changes over the LOR and WEUR are less than half of those in CC. Except over the NA, the ocean CCI trends are small compared to those from the surface data. Discrepancies between the two trends are expected given the differences in sampling and observation techniques. Over the NP, $\Delta\mathrm{CC}/\Delta t$ is positive but the ISCCP trend is negative, perhaps reflecting the difficulty in detecting cirrus from the visible and infrared satellite data when low clouds are prevalent underneath the cirrus. From atlases of cloud co-occurrence (Warren et al. 1986, 1988), it was found that the chance of cirrus occurring over stratus, midlevel clouds, and nimbostratus is 20%–40% more likely over the NP than over the NA. Additionally, cirrus occurs without any other clouds present nearly twice as often over the NA than over the NP. Conversely, cirrus occurs 20% more often over cumulus clouds, which have large areas of clear between them, in the NA than in the NP. Thus, any trends in cirrus coverage detected over the NP with the ISCCP data are likely to be diminished in magnitude relative to those over the NA. The surface observations account for the overlap effects by applying a random overlap correction, but do not misclassify cirrus as some other cloud type. Except for the NP case, the sign of $\Delta\mathrm{CC}/\Delta t$ is consistent with the ISCCP trends for the period common to both suggesting that the trends are not artifacts of the observation methods.

The frequency of clear-sky observations was also computed for the land air traffic regions. Over the United States and WASIA, the frequency of clear skies changed by -1.3% and 1.8% decade^{-1}, respectively. Over EUR and WEUR, clear-sky frequency decreased by 0.6% and 0.7% decade^{-1}, respectively. Thus, over the United States, the increase in cirrus coverage was accompanied by fewer totally clear skies indicating that both the amount and frequency of cirrus coverage increased during the period.

The seasonal variations in CC and CCI trends over the United States (Fig. 4a) are generally consistent with the seasonal variations of contrail occurrence frequency (Minnis et al. 2003), satellite contrail coverage (Palikonda et al. 1999, 2004), and ECON. The greater spring and winter trends are accompanied by maxima in contrail frequency and coverage while all five quantities dip during summer. The greatest discrepancies in the relative seasonal values occur during fall when the CC trend drops slightly, a change more in line with the surface-based contrail frequency variation than with changes in the other quantities. Over WEUR, $\Delta\mathrm{CC}/\Delta t$ averaged 1.0% decade^{-1} during summer and fall and -1.0% decade^{-1} during winter and spring (Fig. 4b), a seasonal variation differing from the satellite-based contrail coverage (Meyer et al. 2002) and ECON. Over WASIA, EUR, and the LOR, $\Delta\mathrm{CC}/\Delta t$ was negative during all seasons except for summer over WASIA. Max-

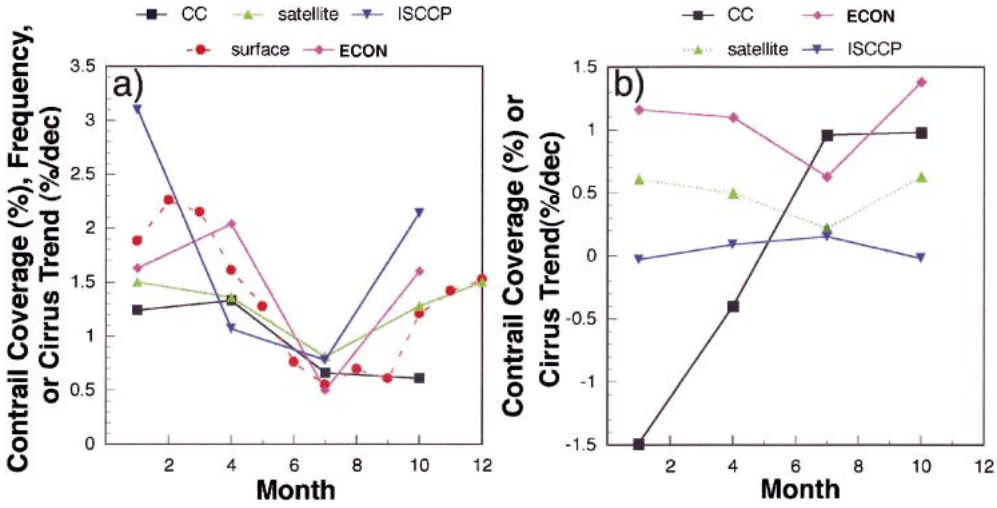

FIG. 4. Seasonal trends in cirrus and contrail amounts and frequencies over (a) the United States and (b) WEUR. The ISCCP and CC lines are cirrus trends. The ECON lines correspond to expected contrail coverage for 1992. Satellite denotes mean linear contrail coverage derived from satellite data during the mid-1990s. Surface data denote persistent contrail frequency observed from the surface during the 1990s. The U.S. winter and spring trends are significant at the 99% confidence level compared to 84% for summer and fall. Only the summer CC trend over WEUR is significant at the 99% confidence level, while the winter and fall trends are significant at the 84% confidence level. The WEUR spring trend is not statistically significant. If cirrus coverage is increasing because of contrail generation, then it should increase proportionately with contrail coverage. This idea is borne out by data over the United States, but not over WEUR.

imum $\Delta CC/\Delta t$ occurred during spring, summer, and fall over the NA, NP, and OOR, respectively.

Because the number of observing sites over the United States decreased during the period, the sensitivity of the CC trends to the number of years sampled was examined to ensure that the 15-yr requirement for using a grid box in the regional analysis did not introduce any artificial trend in the results. The U.S. trends were computed using 20-, 24-, and 25-yr requirements reducing the number of U.S. grid boxes from 104 to 99, 67, and 43, respectively. The corresponding U.S. trends were 0.95%, 1.18%, and 1.11% decade^{-1} indicating that the sampling uncertainty is on the order of 10%–12%. The number of observing sites was generally more stable over other land areas.

b. Humidity impact

Most contrails form between 200 and 300 hPa where often $T < -39$°C. The lowest pressure with Rh reported in the NCEP reanalyses is 300 hPa. When Rhi = 100%, the minimum threshold for cirrus and contrail formation, Rh should be about 68% at −40°C and 60% at −50°C (Fig. 1). Given the known biases and uncertainties in radiosonde Rh measurements at low temperatures (Sassen 1997; Miloshevich et al. 2001), a more conservative estimate of the formation threshold would be 40% at −40°C, and less at lower temperatures. Thus, persistent contrails are likely to form if Rh > 40% and $T < -39$°C as measured from radiosondes, while cirrus clouds are more likely to form at a higher Rh threshold (Ponater et al. 2002). The annual frequency of Rh > 40% at high altitudes should provide a measure of how often cirrus or contrails form or how much area they cover during a given year. Although only the annual mean value of Rh at 300 hPa (RH3) is available from the NCEP data, Minnis et al. (2003) showed that it was highly correlated with the frequency of Rh(300 hPa) > 40% over the United States. Figure 5 shows the regression of RH3 with the annual frequency of Rh(300 hPa) > 40% from radiosonde data at 78 locations in the Comprehensive Aerological Research Data Set (CARDS; see Eskridge et al. 1995). It yields a squared linear correlation coefficient R^2 of 0.94 and shows that RH3 is an excellent predictor of the frequency of humidity levels conducive to contrail and cirrus formation at 300 hPa. Comparisons with radiosonde data (Minnis et al. 2003) show that RH3 is also highly correlated with the frequencies of Rh(250 hPa) and Rh(200 hPa) greater than 40%, yielding R^2 values of 0.74 and 0.52, respectively. Thus, RH3 can be used as a measure of the long-term variations in the frequency of persistent contrail conditions within the typical contrail altitude range.

Radiosondes at a given location may give accurate profiles of Rh instantaneously, but are subject to considerable error in the long term because of instrument changes and variations in reporting practices (Elliot and Gaffen 1991; Gaffen 1993). Over land, NCEP incorporates radiosonde data, adjusting the profiles when necessary to maintain consistency with the model physics (Kistler et al. 2001). Over oceans, only radiosonde data from islands and coastlines are assimilated by NCEP;

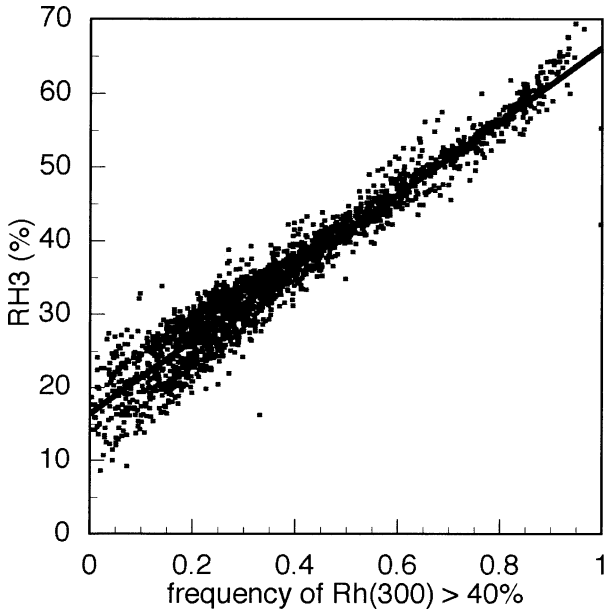

FIG. 5. Variation of RH3 with the frequency of occurrence of Rh(300 hPa) > 40% from CARDS rawinsonde data from 77 stations, 1971–2000. Contrail formation and cirrus persistence are highly probable if Rh(300 hPa) > 40%. Thus, RH3 can serve as a predictor for cirrus persistence.

no other maritime humidity data are used. Comparisons of NCEP RH3 values with those from other sources yield mixed results, but CARDS and NCEP are positively correlated at statistical significance levels of 88% over WASIA and 99% over WEUR, EUR, and LOR (see appendix A). There is no correlation between the two parameters over the United States (see appendix A). NCEP and CARDS are most consistent over Europe where the negative RH3 trend (Fig. 2d) is strongest. The NCEP data used here are currently the best available estimate of UTH over land for the study period (see appendix A).

Trends in RH3, $\Delta\text{RH3}/\Delta t$, are negative everywhere except over the United States (Table 3), where the trend is insignificant. Mean temperatures at 300 hPa are below −39°C everywhere except over the OOR (Table 3). Figure 6 shows scatterplots of and linear regression fits to RH3 and CC data over the land regions. The lack of a RH3–CC correlation over the United States (Fig. 6c) and WEUR (Fig. 6b) indicates that the cirrus variation cannot be explained by the NCEP UTH trends. However, RH3 explains 39%, 46%, and 33% of the variance in CC over WASIA (Fig. 6a), EUR (Fig. 6b), and the LOR (Fig. 6d), respectively, where ECON is relatively small. The slopes of the respective linear fits (Fig. 6) are 0.3, 0.2, and 0.6%CC $(\%\text{RH3})^{-1}$, suggesting that CC is less sensitive to changes in RH3 over EUR, where ECON is relatively large, than over the LOR. Over ocean, CC and RH3 are negatively correlated with R^2 ranging from 0.30 to 0.39 highlighting the large uncertainty in UTH over the oceans. Hereafter, only humidity impacts over land are considered.

TABLE 3. Trends in mean 300-hPa relative humidity from NCEP: 1971–95.

Air traffic region	Trend in RH3 (% decade^{-1})	Mean temperature (K)
WASIA	−3.2	223.1
EUR	−5.0	225.7
WEUR	−6.2	226.7
USA	−0.2	230.5
LOR	−1.2	230.4
NA	−1.8	227.6
NP	−1.7	230.0
OOR	−1.3	235.4

The trend in total cirrus coverage CC can be estimated as the sum of the trend in contrail cirrus and the dependence of natural cirrus coverage c_{nat} on RH3,

$$\frac{\Delta\text{CC}}{\Delta t} = \frac{\Delta c_{\text{nat}}}{\Delta\text{RH3}}\frac{\Delta\text{RH3}}{\Delta t} + \frac{\Delta\text{ECON}}{\Delta t} f_s, \qquad (2)$$

where $\Delta\text{ECON}/\Delta t$ is estimated from ECON (Table 2) and the growth in air traffic (ECON is assumed to be zero in 1970 for WASIA and the LOR). Values of CC increased over the United States despite no change in RH3, while it remained relatively steady over WEUR as RH3 plummeted. Between 1970 and 1995, air traffic increased by factors of 3.7 and 5.2 over the United States and Europe (Penner et al. 1999), respectively, augmenting the respective contrail-forming potentials by approximately 15% and 21% each year relative to 1970 air traffic. If the frequency distribution of Rh remained steady throughout the period, then CC should have increased over those regions. Additional air traffic each year would produce more contrail cirrus for 100% < Rhi < 140% (area B in Fig. 1) while natural cirrus coverage would remain constant, resulting in a net increase in CC as seen for the United States. If the frequency of Rh > 40% decreased each year as indicated by RH3, then natural cirrus coverage would decrease proportionately as seen for the LOR, EUR, and WASIA. A simultaneous rise in air traffic would produce proportionately more contrail cirrus for 100% < Rhi < 140%. In that instance, CC should decrease at a smaller rate than expected for aircraft-free conditions. The amount of counterbalancing would depend on the absolute annual increase in flights and the reduction rate in RH3. Over WEUR, the greater number of flights is apparently sufficient to offset the decrease in RH3, while over WASIA and the LOR, the smaller amount of air traffic would have less impact and is probably insufficient to offset the drop in RH3. Large interannual changes in RH3 can affect the occurrence of both cirrus and contrails (Minnis et al. 2003), but over the long term, increases in air traffic should offset some of the reduction in CC caused by decreases in RH3.

Assuming that ECON increased linearly with air traffic, the correlation between ECON and CC is negative

over the LOR, WASIA, and EUR and near zero over WEUR. A fit to the U.S. data for ECON increasing by 15% yr^{-1} relative to 1971 yields $R^2 = 0.42$. This degree of correlation is comparable to that between RH3 and CC over LOR and EUR. Thus, over the one air traffic region where RH3 appears to be essentially invariant, air traffic can account for changes in CC as well as RH3 can in the air traffic regions where RH3 changes significantly. Over WEUR, a two-parameter fit using RH3 and ECON to predict CC yields a negligible increase (0.0006 to 0.014) in R^2 relative to the correlation in Fig. 6b suggesting that the interannual variability is too large or the dramatic decrease in RH3 during the period had an inordinate impact on the frequency distributions of Rhi.

Any conclusion about the role of aircraft in the U.S. CC trends must consider all of the evidence rather than the humidity trends alone because of the uncertainties in RH3. Prior to 1994, few measurements were taken over the United States when $T < -40$°C. However, CC and RH3 are also uncorrelated over WEUR, where RH3 is consistent with both satellite and radiosonde observations (see appendix A) and ECON is comparable to that over the United States. This similarity supports the absence of an RH3 trend over the United States. The seasonal variations in the U.S. CC trends from both surface and satellite data have the same general characteristics as the magnitudes of the trends in contrail coverage. No statistically significant seasonal trends were found in RH3 over the United States, further suggesting that relative humidity is not responsible for the CC trends. Given the positive CC trends in the surface and satellite observations, the seasonal consistency between contrails and $\Delta CC/\Delta t$, the lack of an RH3 trend, an increase in cirrus frequency, and the known impacts of contrails on cirrus coverage, it is concluded that air traffic is most likely responsible for the 1% $decade^{-1}$ growth in CC over the United States. It appears that cirrus coverage would have diminished over WEUR without the continually increasing high-altitude air traffic. In a similar vein, CC probably would have decreased more over WASIA, the remainder of Europe, and the LOR without contrails. Air traffic probably contributed to the increase of CC over the studied ocean areas. However, without improved estimates of UTH over the ocean, it will be difficult to determine the magnitude of that impact.

Based on the air traffic increase, the estimated linear contrail coverage rose by 0.55% $decade^{-1}$ over the United States compared to the 1% $decade^{-1}$ growth rate in CC. Assuming that the remaining CC increase is due to spreading contrails not detected by satellite analysis, $f_s = 1.8$. If the U.S. case is representative, the maximum impact of linear contrails plus the extra contrail-induced cirrus clouds should be roughly twice that determined for ECON. If the ECON values differ from the actual linear contrail coverage as derived from satellites, then f_s would change accordingly. Assuming that $f_s = 1.8$ for all land areas, the change of natural cirrus with the change in RH3 over EUR, WASIA, and the LOR is estimated to be 0.3, 0.3, and 1.4% $(\%RH3)^{-1}$, respectively. The value for the United States cannot be determined because RH3 was invariant.

c. Climate effects

As of 1999, the ''best'' estimate of maximum net global radiative forcing, $F^{NET} = 0.017$ W m^{-2}, at the top of the atmosphere computed for ECON was based on a contrail optical depth τ of 0.3 and the occurrence of contrails only at a pressure level of 200 hPa (Minnis et al. 1999). Recent studies indicate that, on average, τ is less than 0.30 and the mean contrail pressure is closer to 225 hPa. From satellite measurements, Meyer et al. (2002) found a mean linear contrail optical depth of 0.11 over Europe. Ponater et al. (2002) determined theoretically that the mean global linear contrail optical depth is 0.15 at 250 hPa and is greater over the United States than over Europe. Using satellite data taken over the Midwest, Duda et al. (2004) derived average contrail optical depths of ~0.20 over the life cycles of contrails that developed into cirrus clouds. In a detailed manual analysis of satellite data over the northeastern United States, Minnis et al. (2002) derived a mean optical depth of 0.26 for a large area of contrails from initiation to dissipation. A similar result (mean τ of 0.26) was found by Palikonda et al. (2004) using an automated analysis of linear contrails over the entire United States using data from two satellites during all of 2001. Given the variability in theory and observations, the value of the global mean contrail optical depth remains uncertain but is probably between 0.15 and 0.25 and is likely to be larger over the United States than over Europe.

A new estimate of the potential global radiative forcing by contrails and the resulting cirrus clouds can be made using this new range of optical depths and the spreading factor. Retaining the contrail pressure of 200 hPa assumed by Minnis et al. (1999), the maximum value of F^{NET} ($\tau = 0.25$) including both linear contrails and the resulting contrail-generated cirrus clouds would increase to 0.0255 W m^{-2} because f_s would more than compensate for the reduction in τ from 0.30 to 0.25. Increasing the pressure to 225 hPa would reduce the estimate slightly because the temperature difference between the two levels is approximately 3.5 K. Using $\tau = 0.15$ would reduce the forcing to 0.0153 W m^{-2}. The minimum global estimate of F^{NET} for linear contrails (Marquart and Mayer 2002) is 0.0032 W m^{-2}, a value that would almost double if f_s is considered. Thus, for the combination of contrails and aged-contrail cirrus coverage, the global F^{NET} for 1992 air traffic is most likely between 0.006 and 0.0255 W m^{-2} assuming that f_s is globally representative.

The immediate response to F^{NET} is warming of the atmosphere below the contrail and cooling or warming of the surface depending on the time of day (Meerkötter

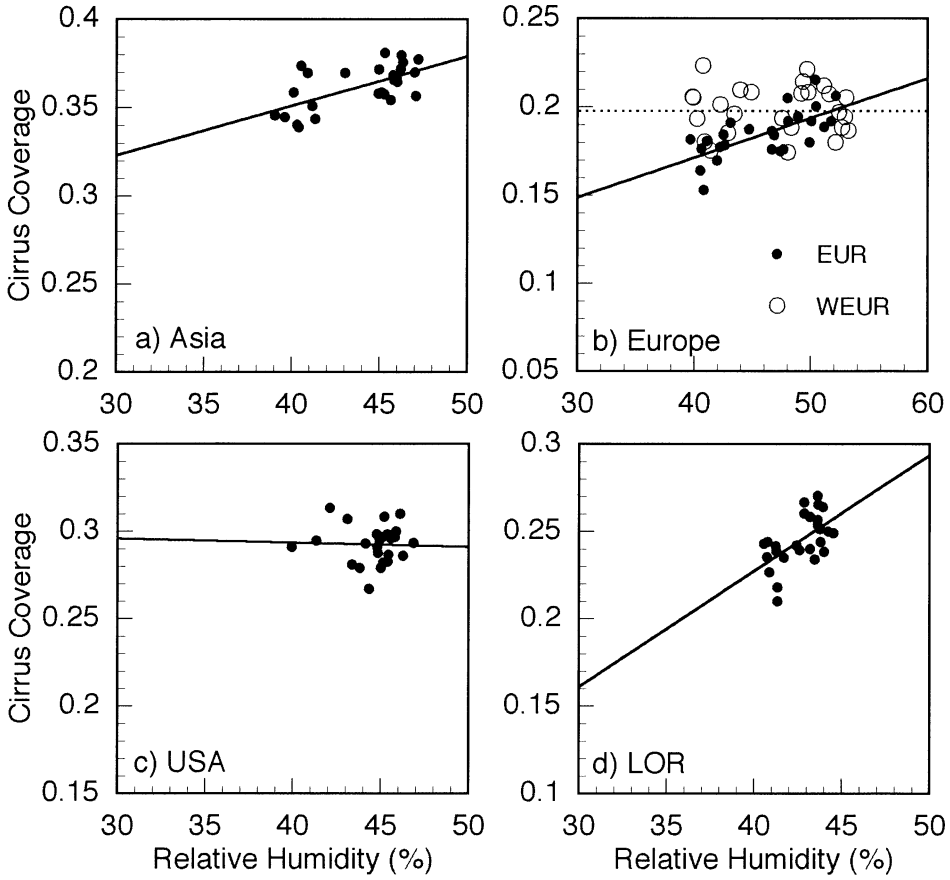

FIG. 6. Correlation of RH3 and mean annual CC, 1971–95, for (a) WASIA, (b) Europe, (c) USA, and (d) LOR.

et al. 1998). Long-term responses to aircraft-induced cirrus have been estimated by inserting small percentages of cirrus into a general circulation model (GCM) at various time steps along the air traffic routes and then running the model to equilibrium (Rind et al. 2000). The GCM results account for many of the feedbacks and the redistribution of the radiative energy in the system. For a 1% change in absolute cirrus coverage with $\tau = 0.33$, the GCM yielded surface temperature changes (ΔT_s) of 0.43° and 0.58°C over the globe and Northern Hemisphere, respectively. The GCM mean tropospheric temperature between 3 and 10 km, ΔT_a, rose by ~0.78°C. The regional variation in $\Delta CC/\Delta t$ (Table 3) and in the RH3 trends would prevent a direct application of the GCM results to estimate the global temperature impact of contrail-induced CC changes. Estimation of the temperature impact of $\Delta CC/\Delta t$ is more straightforward over the United States because the UTH is relatively steady and the CC trend accounts for most of the total cloudiness trend.

The contrail–cirrus effect on the surface and tropospheric temperatures over the United States is estimated

TABLE 4. Tropospheric and surface temperature trends, computed using the observed cirrus trends (cirrus) over the United States and from radiosonde date (labeled Angell) over North America between 20° and 50°N from Angell (1999). Computed results are given for two contrail-cirrus optical depths.

	$\Delta T_a/\Delta t$ (°C decade^{-1})			$\Delta T_s/\Delta t$ (°C decade^{-1})		
	Cirrus			Cirrus		
	$\tau = 0.15$	$\tau = 0.25$	Angell	$\tau = 0.15$	$\tau = 0.25$	Angell
Winter	0.25	0.41	0.46	0.21	0.35	0.43
Spring	0.26	0.44	0.32	0.23	0.38	0.38
Summer	0.13	0.22	0.17	0.11	0.18	0.15
Fall	0.12	0.21	0.19	0.10	0.17	0.13
Annual	0.19	0.32	0.29	0.16	0.27	0.27

using the Rind et al. (2000) values of ΔT_s for the Northern Hemisphere and ΔT_a for the globe. The latter value was used because it was the only tropospheric value available. The temperature trends were computed for the observed U.S. cirrus cover changes as follows:

$$\Delta T/\Delta t = (\tau/0.33)\Delta T\, D\, \Delta \mathrm{CC}/\Delta t, \quad (3)$$

where ΔT is either the surface or tropospheric temperature change for each percent cirrus coverage and the ratio of $\tau/0.33$ accounts for the differences in the contrail optical depths used here and by Rind et al. (2000). Here, D is a correction factor to account for diurnal variability in air traffic and for contrails overlapping clouds. The GCM study did not include the diurnal variation of contrail coverage, which is considerably reduced between 0000 and 0600 local time over the United States (Garber et al. 2004). The GCM also inserted the simulated contrails during clear-sky conditions. The value of D used here is 0.55. Its derivation is described in appendix B and assumes that temperature change is proportional to radiative forcing. The unit radiative forcing for $\tau = 0.25$ is 16.1 W m^{-2}, a value equal to the global maximum value mentioned earlier divided by the total contrail-cirrus coverage. Thus, a 1% increase in contrail coverage over the United States would correspond to $F_{\mathrm{NET}} = 0.16$ W m^{-2}. From (3), the respective surface and air temperature trends over the United States due to $\Delta \mathrm{CC}/\Delta t$ are 0.16° and 0.19°C decade^{-1} if $\tau = 0.15$ and 0.27; and 0.32°C decade^{-1} if $\tau = 0.25$.

Angell (1999) determined the zonal trends in surface and atmospheric temperatures over North America between 1973 and 1994. For comparison with the trends estimated here from the cirrus data, the average temperature trends for the surface and the troposphere between 850 and 300 hPa were taken from the layer means in Figs. 3 and 4 of Angell (1999) for the zones: 40°–50°N, 30°–40°N, and 20°–30°N. The trends for the southernmost zone were given a weight of only 0.5 because the boundaries of the contiguous United States are north of 25°N. The mean annual and seasonal trends (Table 4) computed for $\tau = 0.15$ and 0.25 bound all of the corresponding observations from Angell (1999), except for winter when the observed temperature trends slightly exceed those estimated for $\tau = 0.25$. From the U.S. linear contrail observations noted earlier, it is likely that the appropriate value of τ is closer to 0.25 than to 0.15. The U.S. seasonal ΔT_a trends are opposite those for the entire Northern Hemisphere where the weakest increases in temperature occur during winter and early spring, and the mean annual hemispheric trends are less than half those over the United States (Pielke et al. 1998). These results demonstrate that the increased cirrus coverage, attributable to air traffic, could account for nearly all of the surface and tropospheric warming observed over the United States between 1975 and 1994. They should not be extrapolated to conclude that contrails are responsible for warming in other regions.

The value of F^{NET}, 0.16 W m^{-2} (%CC)$^{-1}$, for the United States estimated from the modified results of Minnis et al. (1999) corresponds to a 0.32°C decade^{-1} trend in temperature (Table 4). These values suggest that a 1°C temperature change results from a 0.5 W m^{-2} top-of-the-atmosphere forcing, a response-forcing ratio of 2.0. Because the radiative forcing at the tropopause is slightly larger than that at the top of the atmosphere (Ponater et al. 2002), the response ratio would be somewhat smaller. The results from Rind et al. (2000) indicate that the response ratio for F^{NET} at the tropopause is highly variable. For a cirrus increase of 0.4%, the response ratios are 1.7 and 3.0 for the Northern Hemisphere and the globe, respectively. The respective values for an increase of ~1.3% are 0.75 and 1.5. Thus, the results in Table 4 are reasonable given the estimated radiative forcing.

The actual response to increased cirrus coverage via contrails, however, is not likely to be in the equilibrium state used by the GCM. Contrail outbreaks are more sporadic than the regular insertion technique used by Rind et al. (2000) and the steadily increasing air traffic does not allow the actual atmospheric system to reach an equilibrium. The instantaneous response would also not be appropriate because of the long time period considered and the tendency of significant contrails to last many hours and occur at different times of day. The results in Table 4 assume that the system response occurs in the region of the radiative forcing. The Rind et al. (2000) equilibrium study shows that the heating by contrails is often displaced from the location of the contrail insertion. It remains uncertain, without more realistic modeling of the contrail behavior, whether the long-term temperature change will occur in the region where the cirrus coverage increases or whether it is displaced and smoothed by the global circulation.

5. Concluding remarks

The estimated temperature changes are based on a simple application of limited GCM calculations and assume that cirrus coverage is the only parameter changing during the period. Other GCM formulations may yield different results than the Rind et al. (2000) study used here. Changes in aerosol concentrations, greenhouse gases, and the geographical distribution of clouds, as well as other air traffic effects, were not taken into account. For example, ozone formed from air traffic exhaust is expected to produce a positive radiative forcing comparable to that from contrails and would result in additional tropospheric warming below the flight levels (Penner et al. 1999). Also, contrails that form in existing cirrus clouds and do not contribute additional cloud cover can increase the cirrus optical depth further affecting F^{NET}. Despite the good correlations between RH3 and CC outside of heavy air-traffic land areas, UTH estimates must be viewed with some skepticism because filtering of observations may have eliminated significant portions of the soundings available for assimilation by

the NCEP model. Better measurements of UTH, cloud distributions, and contrail properties, and more precise specification of flight paths and improved parameterizations of cirrus and contrail formation in GCMs are needed to more rigorously determine the contrail climate impacts. This study indicates that contrails already have substantial regional effects where air traffic is heavy. As air travel continues growing in other areas, the impact may become globally significant.

Acknowledgments. Many thanks to D. Young and D. Duda for critical reviews, U. Schumann and D. Fahey for their comments, K. Gierens for providing the contrail distributions, C. Hahn for assistance with the cirrus data, D. Doelling for assistance in analyzing the radiosonde data, and D. Minnis for continued encouragement. This research was supported by the NASA Office of Earth Science Pathfinder Program under NRA-99-OES-04.

APPENDIX A

Evaluation of Relative Humidity Data

When compared with satellite estimates of UTH, radiosonde measurements of Rh are overestimated for the former Soviet Union and China and underestimated over the United States and western Europe (Soden and Lanzante 1996). The satellite–radiosonde discrepancies were attributed to the use of different types of humidity instruments. Relative to the CARDS values, the NCEP reanalyses reduced RH3 over Asia (Fig. A1a) and increased RH3 over Europe (Fig. A1b) and the United States (Fig. A1c). Over other parts of the globe, RH3 increased by ~15% compared to the CARDS values (Fig. A1d). The NCEP trends are consistent with the CARDS data over Europe and the rest of the globe. Over the United States, the CARDS data show a rise

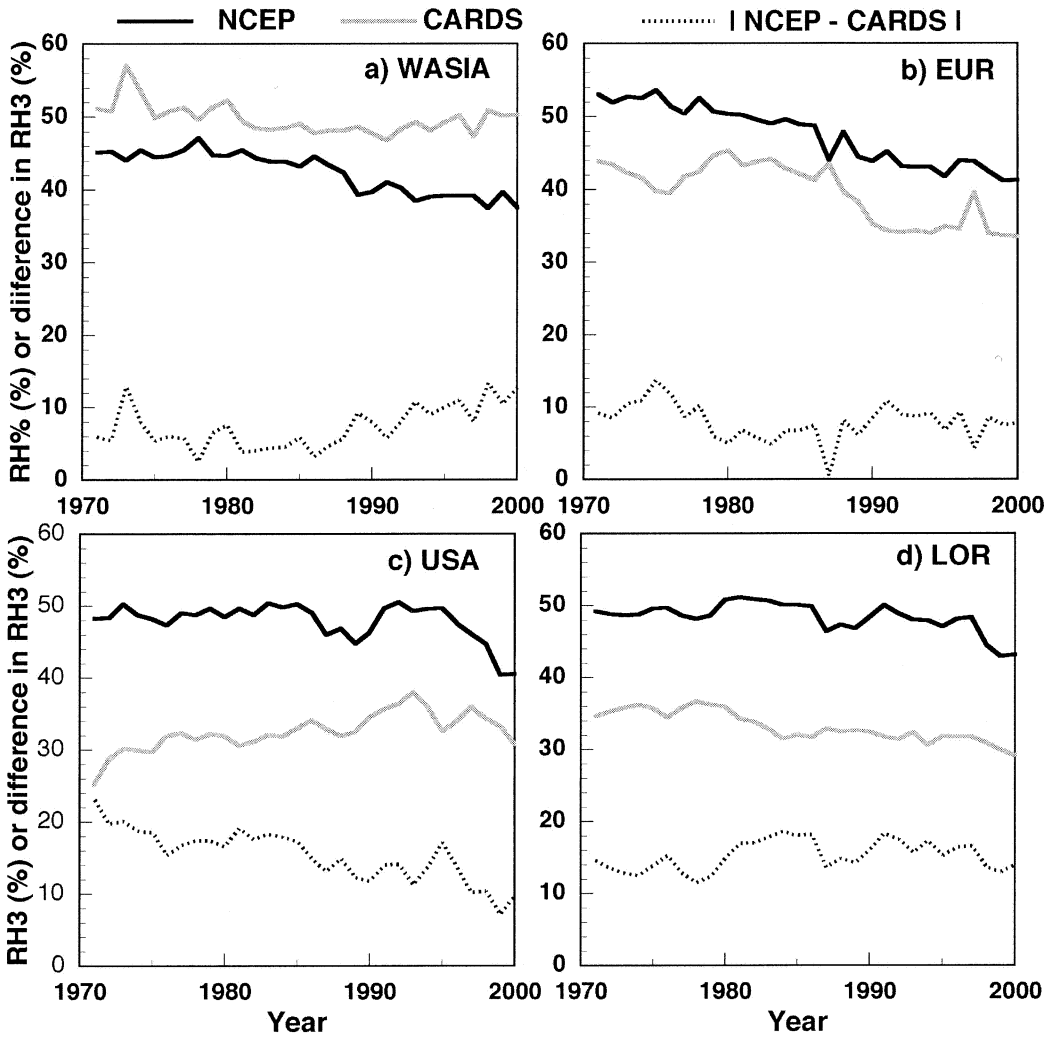

FIG. A1. Comparisons of annual mean 300-hPa relative humidities over CARDS sites within the air traffic regions (a) WASIA, (b) EUR, (c) USA, and (d) LOR. The dashed line shows the absolute value of the difference between the two estimates of RH3.

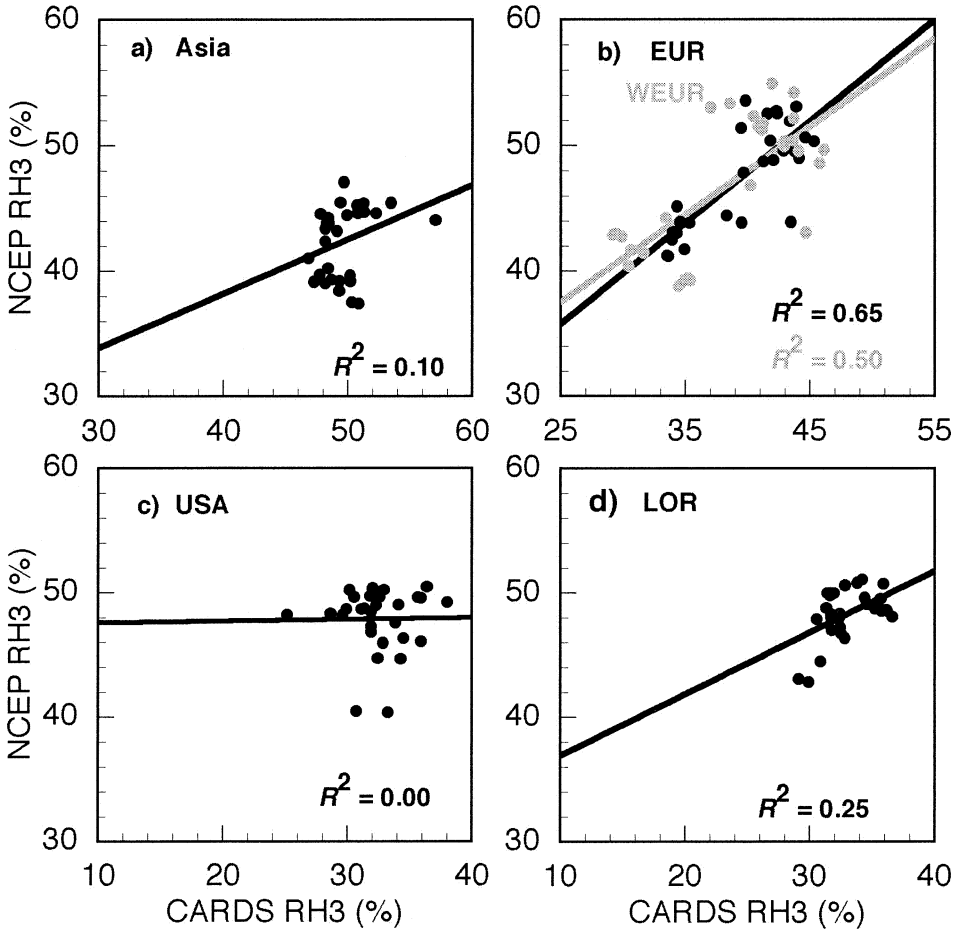

FIG. A2. Correlations of RH3 data shown in Fig. A1.

in RH3 with year, while the NCEP RH3 shows no significant trend. The U.S. CARDS RH3 values are probably the least reliable of considered datasets, however, because only 65% of the 104 419 soundings taken between 1971 and 2000 that had a valid Rh at 400 hPa also had a valid Rh at 300 hPa. Furthermore, only 25% of the 400-hPa valid soundings had a valid Rh when $T < 233$ K. Prior to October 1993, Rh was not reported for $T < 233$ K and it was set equal to 19% whenever the measured value was less than 20% (Elliott et al. 1998). Most of the valid cold Rh values occurred after 1993 when reporting practices began to include Rh at all levels regardless of temperature (Elliott et al. 2002). A variety of other problems plague the U.S. radiosonde record (Eskridge et al. 1995; Elliott et al. 1998, 2002). Since the NCEP reanalysis adjusts values to achieve model consistency and computes Rh(300 hPa) for all temperatures, it is not surprising that the NCEP and CARDS RH3 trends are different. Valid Rh(300 hPa) values occurred 84%, 77%, and 77% of the time over WASIA, Europe, and the rest of globe, respectively, in the CARDS data when T(300 hPa) < 233 K and Rh(400 hPa) was valid.

The CARDS and NCEP RH3 values are well correlated over EUR, WEUR, and OOR, but not over WASIA or over the United States (Fig. A2). Over Asia, RH3 from NCEP and CARDS diverge after 1986 resulting in the diminished correlation between NCEP and the CARDS RH3. Documentation of the radiosonde data taken over WASIA (Elliott and Gaffen 1991) does not indicate any significant changes around 1986. However, the statistically significant decrease in CC over WASIA (Table 2) supports the negative trend in RH3 suggesting the possibility of some unreported changes in instrumentation or reporting practices in one or more reporting countries. The lack of correlation over the United States is not surprising because the CARDS profiles lack values for most of the cold seasons as discussed earlier.

The greatest values of CC occur over WASIA suggesting that RH3 should be larger there than in any other air traffic region. Because the dry bias in the measurements depends on temperature, the measurements and, hence, the NCEP RH3 values would be lower than over other regions because the 300-hPa temperature (Table 2) is 7 K less than anywhere else. An empirical correction formula (Minnis et al. 2002) indicates that at

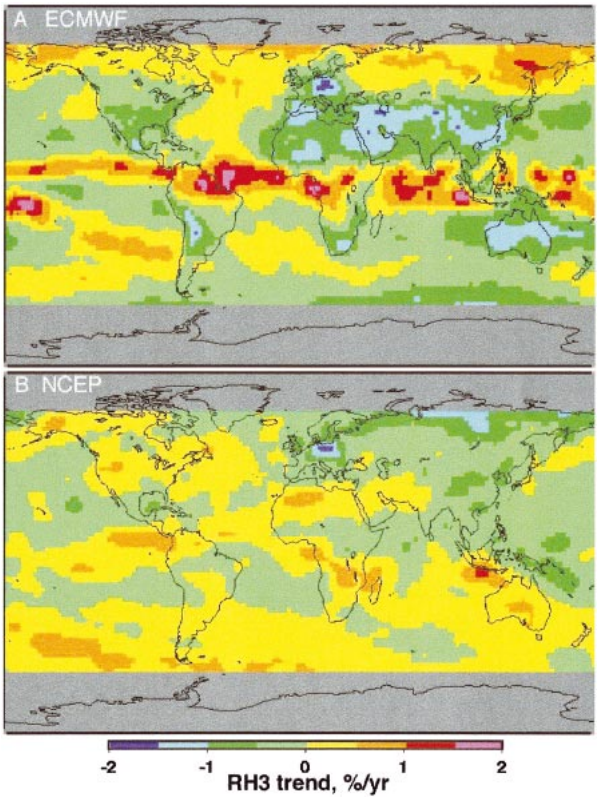

FIG. A3. The 1985–96 trends in RH3 from (a) ECMWF and (b) NCEP reanalyses.

223 K, the measured Rh would be nearly 21% less than the true value at ice saturation compared to that at 230 K, which would be only 14% less than the corresponding true value at ice saturation. If such biases hold for the NCEP data, then approximately 7% should be added to the RH3 values over Asia resulting in the Asian values exceeding their U.S. counterparts. Given the poor state of UTH measurements and their use in assimilation models, it is not expected that the absolute value of RH3 will be highly accurate for a given region.

Trends in RH3 and in the average RH between 300 and 500 hPa were computed for 1979–98 for comparison with satellite-derived values of UTH (Bates and Jackson 2001). A comparison with Fig. 1 from Bates and Jackson (2001) indicates that the NCEP trends are generally opposite in sign to those from the satellite data over most land areas. Better agreement was found over the oceans. The trends in RH3 from NCEP were also compared to those from the European Centre for Medium Range Forecasts (ECMWF) monthly Tropical Ocean Global Atmosphere (TOGA) Global Tropospheric Analyses for 1985–96 (Fig. A3) when ECMWF data are available (ECMWF 1995). In general, the ECMWF trends are more extreme than their NCEP counterparts. They agree in sign over Europe, western Asia south of 50°N, and over much of the NP and NA. The trends are opposite in sign over many other areas including the United States and Australia. The NCEP trends are only significant at the 90% confidence level over the western United States, Europe, Siberia, China, and Australia. The ECMWF trends are significant over the eastern United States, Europe, China, southern Asia, Siberia, and Australia. Thus, the two datasets show some significant disagreement. Both datasets were correlated with CC for the various air traffic regions. The values of R^2 for the ECMWF RH3 were all less than 0.12 and none of the correlations were statistically significant.

The only UTH data available for 1971–96 are from CARDS or NCEP. ECMWF reanalyses are not yet available for the entire time period. Of all of the data available for any significant time period, only the NCEP RH3 values show significant correlations with CC for areas where contrails should play a minor role in cirrus coverage. The correlations over ocean are significant but of the wrong sign. Further study is needed to understand this behavior over oceans. The CARDS data are available only over a limited number of sites and overall are not correlated with CC any better than the NCEP data. Thus, because of data quality, consistency, and coverage, the NCEP dataset is the best available for comparison with the CC trends. From all of the available evidence, however, it appears that the NCEP data over land make the most sense and, therefore, constitute the most appropriate UTH dataset for the study period or any significant portion of it.

APPENDIX B

Determination of Diurnal and Cloud Correction Factor for Estimating Contrail-Induced Temperature Changes

If it is assumed that radiative forcing is directly proportional to a temperature change, then radiative forcing values can be used to establish the desired correction factor D to account for the lack of an air traffic diurnal cycle and the absence of contrail–cloud overlap in the Rind et al. (2000) estimates of temperature change due to contrails. Here, D is estimated using the global radiative forcing results for $\tau = 0.3$ in Table 1 from Minnis et al. (1999), which included an air traffic diurnal cycle and overlapping clouds and contrails. The shortwave (SW), longwave (LW), and net radiative forcings from Minnis et al. (1999) are $F_d^{\mathrm{SW}} = -0.008$, $F_d^{\mathrm{LW}} = 0.025$, and $F_d^{\mathrm{NET}} = 0.017$ W m^{-2}, respectively.

The absence of a diurnal cycle in the GCM results only affects the longwave forcing. Air traffic over the United States during the night is roughly 42% of that during the day (Garber et al. 2004). Assuming that day and night are 12 h each and that the unit nighttime LW radiative forcing over land ($F_{\mathrm{nite}}^{\mathrm{LW}}$) is 90% of that during the day due to heating and cooling of the surface, the total LW forcing accounting for a diurnal cycle in air traffic is

$$0.025 = 0.5F_{\mathrm{day}}^{\mathrm{LW}} + 0.5 \times 0.42 \times 0.9F_{\mathrm{day}}^{\mathrm{LW}}, \quad \text{(B1)}$$

where F^{LW}_{day} is the daytime LW forcing. Solving (B1) yields $F^{LW}_{day} = 0.0363$ W m^{-2} and $F^{LW}_{nite} = 0.0326$ W m^{-2}. If the air traffic was constant as in Rind et al. (2000), then the total radiative forcing would be

$$F^{LW}_r = 0.5\ F^{LW}_{day} + 0.5\ F^{LW}_{nite}. \quad \text{(B2)}$$

Thus, $F^{LW}_{rd} = 0.0345$, a value that is 38% greater than that for a day–night ratio of 2.4. Assuming random cloud overlap, the SW and LW radiative forcings from Minnis et al. (1999) can be approximated as

$$F^{SW}_d = F^{SW}_{clr}(1 - A_c) + A_c F^{SW}_{cld} \quad \text{and} \quad \text{(B3)}$$

$$F^{LW}_d = F^{LW}_{clr}(1 - A_c) + A_c F^{LW}_{cld}, \quad \text{(B4)}$$

respectively. The subscripts, cld and clr refer to cloudy and clear areas, respectively, and A_C is the mean cloud fraction. The relative clear and cloudy forcings were estimated using the results from Fig. 5 of Meerkötter et al. (1999) that show the unit radiative forcings for a clear scene and for the same scene with a low-level cloud. The unit SW forcings for the clear and cloudy scenes are -14 and -2 W m^{-2}, respectively. Thus,

$$F^{SW}_{cld} = 0.14\ F^{SW}_{cld}. \quad \text{(B5)}$$

Assuming an average cloud height of 5 km over the United States and a linear variation of F^{LW}_{cld} with cloud height, the unit LW radiative forcing at 5 km in the Meerkötter et al. (1999) would be 31 W m^{-2} compared to 57 W m^{-2} for the clear case and

$$F^{LW}_{cld} = 0.54\ F^{LW}_{clr}. \quad \text{(B6)}$$

Substituting (B5) and (B6) into (B3) and (B4), respectively, and assuming A_C is 50%, F^{SW}_{clr} and F^{LW}_{clr} are -0.0140 and 0.0325 W m^{-2}, respectively. Thus, in the absence of cloud cover and the air traffic diurnal cycle,

$$F^{LW}_r = 1.38F^{LW}_{clr}, \quad \text{and} \quad \text{(B7)}$$

$$F^{SW}_r = F^{SW}_{clr}. \quad \text{(B8)}$$

The equivalent net forcing for the GCM case, F^{NET}_r, is the sum of (B7) and (B8), which produces a value of 0.0309 W m^{-2}. The correction factor D is simply the ratio of F^{NET}_d to F^{NET}_r, which yields a value 0.55.

REFERENCES

Angell, J. K., 1999: Variation with height and latitude of radiosonde temperature trends in North America, 1975–94. *J. Climate,* **12,** 2551–2561.

Bates, J. J., and D. L. Jackson, 2001: Trends in upper-tropospheric humidity. *Geophys. Res. Lett.,* **28,** 1695–1698.

Boucher, O., 1999: Air traffic may increase cirrus cloudiness. *Nature,* **397,** 30–31.

Changnon, S. A., 1981: Midwestern cloud, sunshine and temperature trends since 1901: Possible evidence of jet contrail effects. *J. Appl. Meteor.,* **20,** 496–508.

Duda, D. P., P. Minnis, and L. Nguyen, 2001: Estimates of cloud radiative forcing in contrail clusters using GOES imagery. *J. Geophys. Res.,* **106,** 4927–4937.

——, ——, ——, and R. Palikonda, 2004: A case study of the development of contrail clusters over the Great Lakes. *J. Atmos. Sci.,* in press.

ECMWF, cited 1995: The description of the ECMWF/WCRP Level III—A global atmospheric data archive. [Available online at http://www.ecmwf.int/products/data/archive/descriptions/od/toga/.]

Elliott, W. P., and D. J. Gaffen, 1991: On the utility of radiosonde humidity archives for climate studies. *Bull. Amer. Meteor. Soc.,* **72,** 1507–1520.

——, R. J. Ross, and B. Schwartz, 1998: Effects on climate records of changes in National Weather Service humidity processing procedures. *J. Climate,* **11,** 2424–2436.

——, ——, and W. H. Blackmore, 2002: Recent changes in NWS upper-air observations with emphasis on changes from VIZ to Vaisala radiosondes. *Bull. Amer. Meteor. Soc.,* **83,** 1003–1017.

Eskridge, R. E., O. A. Alduchov, I. V. Chernykh, P. Zhai, A. C. Polansky, and S. R. Doty, 1995: A Comprehensive Aerological Reference Dataset (CARDS): Rough and systematic errors. *Bull. Amer. Meteor. Soc.,* **76,** 1759–1775.

Gaffen, D. J., 1993: Historical changes in radiosonde instruments and practices. WMO/TD-No. 541, World Meteorological Organization, 123 pp.

Garber, D. P., P. Minnis, and P. K. Costulis, 2004: A USA commercial flight track database for upper tropospheric aircraft emission studies. *Proc. European Conf. on Aviation, Atmosphere, and Climate,* Friedrichshafen at Lake Constance, Germany, Institut für Physik der Atmosphäre, DLR, in press. [Available online at http://www-5pm.larc.nasa.gov/sass/pub/conference/Garber.AAC.03.pdf.]

Gierens, K., U. Schumann, M. Helten, H. Smit, and A. Marenco, 1999: A distribution law for relative humidity in the upper troposphere and lower stratosphere derived from three years of MOZAIC measurements. *Ann. Geophys.,* **17,** 1218–1226.

Hahn, C. J., and S. G. Warren, 1999: Extended edited synoptic cloud reports from ships and land stations over the globe, 1952–1996. NDP026C, Carbon Dioxide Information Analysis Center, Oak Ridge National Laboratory, Oak Ridge, TN, 80 pp.

Hansen, J., M. Sato, and R. Ruedy, 1997: Radiative forcing and climate response. *J. Geophys. Res.,* **102,** 6831–6864.

Jensen, E., and O. Toon, 1994: Ice nucleation in upper troposphere: Sensitivity to aerosol number density, temperature, and cooling rate. *Geophys. Res. Lett.,* **21,** 2019–2022.

——, and Coauthors, 2001: Prevalence of ice-supersaturated regions in the upper troposphere: Implications for optically thin ice cloud formation. *J. Geophys. Res.,* **106,** 17 253–17 266.

Kistler, R., and Coauthors, 2001: The NCEP–NCAR 50-Year Reanalysis: Monthly means CD-ROM and documentation. *Bull. Amer. Meteor. Soc.,* **82,** 247–267.

Marquart, S., and B. Mayer, 2002: Towards a reliable GCM estimation of contrail radiative forcing. *Geophys. Res. Lett.,* **29**, 1179, doi: 10.1029/2001GL014075.

Meerkötter, R., U. Schumann, D. R. Doelling, P. Minnis, T. Nakajima, and Y. Tsushima, 1999: Radiative forcing by contrails. *Ann. Geophys.,* **17,** 1070–1084.

Meyer, R., H. Mannstein, R. Meerkötter, U. Schumann, and P. Wendling, 2002: Regional radiative forcing by line-shaped contrails derived from satellite data. *J. Geophys. Res.,* **107**, 4104, doi:10.1029/2001JD000426.

Miloshevich, L. M., H. Vömel, A. Paukkunen, A. J. Heymsfield, and S. J. Oltmans, 2001: Characterization and correction of relative humidity measurements from Vaisala RS80-A radiosondes at cold temperatures. *J. Atmos. Oceanic Technol.,* **18,** 135–156.

Minnis, P., D. F. Young, L. Nguyen, D. P. Garber, W. L. Smith Jr., and R. Palikonda, 1998: Transformation of contrails into cirrus during SUCCESS. *Geophys. Res. Lett.,* **25,** 1157–1160.

——, U. Schumann, D. R. Doelling, K. Gierens, and D. Fahey, 1999: Global distribution of contrail radiative forcing. *Geophys. Res. Lett.,* **26,** 1853–1856.

——, L. Nguyen, D. P. Duda, and R. Palikonda, 2002: Spreading of isolated controls during the 2001 air traffic shutdown. Preprints,

10th Conf. on Aviation, Range, and Aerospace Meteorology, Portland, OR, Amer. Meteor. Soc., J9–J12.

——, J. K. Ayers, S. P. Weaver, and M. L. Nordeen, 2003: Contrail frequency over the United States from surface observations. *J. Climate*, **16,** 3447–3462.

Nakanishi, S., J. Curtis, and G. Wendler, 2001: The influence of increased jet airline traffic on the amount of high level cloudiness in Alaska. *Theor. Appl. Climatol.*, **68,** 197–205.

Palikonda, R., P. Minnis, D. R. Doelling, P. W. Heck, D. P. Duda, H. Mannstein, and U. Schumann, 1999: Contrail climatology over the USA from MODIS and AVHRR data. Preprints, *10th Conf. on Atmospheric Radiation*, Madison, WI, Amer. Meteor. Soc., 181–184.

——, D. N. Phan, V. Chakrapani, and P. Minnis, 2004: Contrail coverage over the USA from MODIS and AVHRR data. Preprints, *European Conf. on Aviation, Atmosphere, and Climate*, Friedrichshafen at Lake Constance, Germany, Institut für Physik der Atmosphäre, DLR, in press. [Available online at http://www-pm.larc.nasa.gov/sass/pub/conference/rabi.AAC.03.pdf.]

Penner, J. E., D. H. Lister, D. J. Griggs, D. J. Dokken, and M. McFarland, Eds., 1999: *Aviation and the Global Atmosphere.* Cambridge University Press, 373 pp.

Pielke, R. A., J. Eastman, T. N. Chase, J. Knaff, and T. G. F. Kittel, 1998: 1973–1996 trends in depth-averaged tropospheric temperature. *J. Geophys. Res.*, **103,** 16 927–16 933.

Ponater, M., S. Marquart, and R. Sausen, 2002: Contrails in comprehensive global climate model: Parameterization and radiative forcing results. *J. Geophys. Res.*, **107**, 4164, doi:10.1029/2001JD000429.

Rind, D., P. Lonergan, and K. Shah, 2000: Modeled impact of cirrus cloud increases along aircraft flight paths. *J. Geophys. Res.*, **105,** 19 927–19 940.

Rossow, W. B., and R. A. Schiffer, 1999: Advances in understanding clouds from ISCCP. *Bull. Amer. Meteor. Soc.*, **80,** 2261–2287.

Sassen, K., 1997: Contrail-cirrus and their potential for regional climate change. *Bull. Amer. Meteor. Soc.*, **78,** 1885–1903.

——, and G. C. Dodd, 1989: Haze particle nucleation simulations in cirrus clouds, and application for numerical and lidar studies. *J. Atmos. Sci.*, **46,** 3005–3014.

Sausen, R., K. Gierens, M. Ponater, and U. Schumann, 1998: A diagnostic study of the global coverage by contrails. Part I: Present day climate. *Theor. Appl. Climatol.*, **61,** 127–141.

Soden, B. J., and J. R. Lanzante, 1996: An assessment of satellite and radiosonde climatologies of upper-troposheric water vapor. *J. Climate*, **9,** 1235–1250.

Ström, J., and Coauthors, 2003: Cirrus cloud occurrence as function of ambient relative humidity: A comparison of observations from the Southern and Northern Hemisphere midlatitudes obtained during the INCA experiment. *Atmos. Chem. Phys. Discuss.*, **3,** 3301–3333.

Travis, D., A. Carleton, and R. Lauritsen, 2002: Contrails reduce daily temperature range. *Nature*, **418,** 601.

Udelhofen, P., and R. D. Cess, 2001: Cloud cover variations over the United States: An influence of cosmic rays or solar variability? *Geophys. Res. Lett.*, **28,** 2617–2620.

Warren, S. G., C. J. Hahn, J. London, R. M. Chervin, and R. L. Jenne, 1986: Global distribution of total cloud cover and cloud type amounts over land. National Center for Atmospheric Research Tech. Note TN-273+STR, 29 pp.

——, ——, ——, ——, and ——, 1988: Global distribution of total cloud cover and cloud type amount over the ocean. National Center for Atmospheric Research Tech. Note TN-317+STR, 42 pp.